INSTITUTE OF PHYSICS PUBLISHING PHYSICS IN MEDICINE AND BIOLOGY

Phys. Med. Biol. **51** (2006) 4719–4733 doi:10.1088/0031-9155/51/18/017

Mean time-of-flight of photons in transillumination measurements of optically anisotropic tissue with an inclusion

Olga K Dudko[1], **George H Weiss**[1] **and Victor Chernomordik**[2]

[1] Mathematical and Statistical Computing Laboratory, Division of Computational Bioscience, Center for Information Technology, National Institutes of Health, Bethesda, MD 20892, USA
[2] Laboratory of Integrative and Medical Biophysics, National Institute of Child Health and Human Development, National Institutes of Health, Bethesda, MD 20892, USA

Received 8 March 2006, in final form 25 July 2006
Published 5 September 2006
Online at stacks.iop.org/PMB/51/4719

Abstract

We study the effect of optical anisotropy on the mean time-of-flight of photons in a slab of turbid medium containing an inclusion whose optical properties differ from those of the bulk. For this analysis the difference in the mean time for a photon introduced into the slab to reach a specified target point with and without the inclusion is calculated. This difference is defined to be a measure of the contrast. The theoretical model is based on a continuous-time random walk on a lattice, which can be solved exactly and furnishes an exact expression for the contrast. Qualitative and quantitative characteristics of the contrast are analysed as functions of the geometric configuration of the system components (locations of the source, the inclusion and the detector), parameters that specify the optical anisotropy of the medium, and either the scattering properties of the inclusion or the lifetime of the small fluorophore in the case of the time-resolved fluorescence experimental configuration.

1. Introduction

The notion of contrast is central to any imaging modality since the purpose of imaging is to detect and identify regions in which some physical property in the body differs from that of its surroundings. Thus, many investigations aim to quantify contrast, as expressed in terms of the effects of absorption and scattering coefficients that differ, in some local region, from those of surrounding tissue. Such an approach has been applied to the analysis of data in a number of recent papers, using as a forward model either diffusion theory, e.g., Michielsen *et al* (1998), Painchaud *et al* (1999), Morin *et al* (2000), or random walk theory, e.g., Gandjbakhche *et al* (1994, 1996, 1998), and Chernomordik *et al* (2002). All are based on an assumption that optical parameters are isotropic throughout the tissue which means that there is no preferred direction associated with photon migration. Nevertheless, it is known that there are many

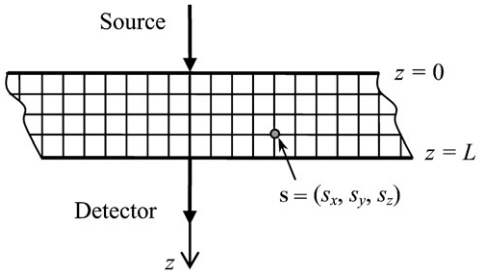

Figure 1. A schematic diagram of a transillumination measurement in which photons from a laser source traverse a slab, emerging on the opposite side. The aim of the measurement is that of measuring the change in the average traversal time induced by an inclusion at $\mathbf{s} = (s_x, s_y, s_z)$ with scattering properties differing from those on the remaining lattice sites. For simplicity the diagram is drawn in two dimensions, and the tissue is modelled as a simple cubic lattice bounded by two parallel absorbing planes.

tissues for which photons tend to migrate preferentially along fibres when these exist, as is true for example, for skin (Nickell *et al* 2000) and white matter in brain, collagen and dentin (Kienle *et al* 2003) and human skeletal muscle (Binzoni *et al* 2006). The most common geometries of aligned fibres correspond either to their orientation being parallel to the surface being illuminated (skin, muscle) or perpendicular to this surface (brain white matter). An early theoretical formulation of diffusion that incorporates effects of anisotropy is to be found in a paper by Heino *et al* (2002).

Our ultimate goal in the present paper is to find, for the transillumination geometry, a simple expression that describes the change in the mean time-of-flight (MTOF) due to the presence of a small inclusion that modifies the time at which photons are detected (either the result of a scattering perturbation or a fluorescence lifetime). The first moment of the flight time can easily be estimated from time-resolved data and is robust due to the suppression of noise that is a result of the integration with respect to time. Use of this parameter was suggested in Arridge (1995) and applied to the analysis of experimental data generated from isotropic tissue-like phantoms in Hebden *et al* (1999) and Arridge *et al* (2000). To avoid misunderstanding it is worth noting that the contrast function used for analysing experimental data in diffuse optical imaging is usually determined as a relative perturbation of light intensity due to the presence of the inclusion (see, e.g., Hebden and Arridge (1996), Gandjbakhche *et al* (1998)). However, here we plan to estimate not the variation in intensity but the MTOF that results from the presence of the inclusion.

We base our analysis on a simplified model of anisotropy first discussed by Dagdug *et al* (2003) and partially verified experimentally in Hebden *et al* (2004) and Sviridov *et al* (2005). Our analysis generalizes formalism developed by Weiss and Calabrese (1996) which dealt with related questions for diffusion in an unbounded space.

2. The model

2.1. The lattice model

The model, in terms of which we frame the analysis, consists of a slab of infinite extent and width L as shown in figure 1. Its planar boundaries are assumed to be perfectly transmitting. By this we mean that a photon reaching the surface emerges as a detectable flash of light at

the time of arrival, thereafter leaving the system. An arbitrary point in the slab will be denoted by $\mathbf{r} = (x, y, z)$, whose components are integers which satisfy $-\infty < x, y < \infty, 0 \leqslant z \leqslant L$. The units measure distances as integer multiples of the scattering length, z_0, which is $\sqrt{2}/\mu_s'$, where μ_s' is the transport-corrected scattering coefficient. A tacit assumption underlying our analysis is that $L \gg z_0$. Without this assumption the validity of a random walk model is questionable since forward scattering effects might then be important. Our analysis will be based on the continuous-time random walk (CTRW) as described in Weiss (1994) and Hughes (1995). This is a random walk in which the times between successive steps are identically distributed random variables.

Two types of distinctions will be made. The first accounts for the distinction between properties of a random walk on a bulk point. A bulk point is defined to be any point on the lattice aside from the inclusion, and the random walk at the point or points of the inclusion. We consider the simplest possible case in which the inclusion consists of a single point $\mathbf{s} = (s_x, s_y, s_z)$. The second distinction is defined by parameters that determine the optical anisotropy.

2.2. *Differences between pausing-time densities as a measure of tissue inhomogeneity*

We define the pausing-time density for a single sojourn by a random walk on a point in the bulk to be equal to $\psi_b(t)$. By this we mean that $\psi_b(t)\,dt$ is the probability that a random walk arriving at a bulk point waits for a time between t and $t + dt$ before making the succeeding step. A random walk arriving at $\mathbf{s}$ is characterized by a different pausing-time density, $\varphi_i(t)$, which is not necessarily equal to $\psi_b(t)$. In this terminology $\varphi_i(t) = \lim_{T\to\infty} \delta(t - T)$ corresponds to a completely absorbing point. The difference between the two pausing-time densities, $\psi_b(t)$ and $\varphi_i(t)$, is the sole distinction made between the inclusion and the bulk points.

A random walk theory, in this framework, provides an advantage over a diffusion theory analysis, since when the propagator for the random walk in discrete time can be found, it is readily converted into a solution in Laplace transform space, which, in turn, can be converted into a solution in continuous time. This is done by replacing the generating function parameter by the Laplace transforms of the appropriate densities $\psi_b(t)$ and $\varphi_i(t)$. A further advantage in discussing the discrete-time model initially is that there is no difference between the models with and without an inclusion since, by our earlier assumption, the degree of inhomogeneity is based on differences only between the pausing-time densities. In the present analysis we will neglect the effects of possible inhomogeneity in internal absorption.

2.3. *Definition of optical anisotropy*

The degree of anisotropy will be characterized by three probabilities, α, β and γ. Each of these is the probability of making a step in one of six possible directions. For simplicity we restrict our analysis to nearest-neighbour random walks, so that a random walk at site $\mathbf{r}$ can only step to one of its six neighbouring points, $(x \pm 1, y \pm 1, z \pm 1)$. The assumption will be made that the probability that a step $x \to x + 1$ or $x \to x - 1$ is made is defined to be α, the probability that the step $y \to y + 1$ or $y - 1$ is made is β and so on, so that $2\alpha + 2\beta + 2\gamma = 1$. Isotropy therefore corresponds to the choice $\alpha = \beta = \gamma = 1/6$, any other choice indicating some degree of anisotropy.

As in Dagdug *et al* (2003) we consider only the two simplified cases defined by $\alpha = \beta \neq \gamma$ and $\beta = \gamma \neq \alpha$. The first of these, $\alpha = \beta$, implies rotational symmetry around the z-axis, while the second corresponds to rotational symmetry around the x-axis. These may be

considered to be two extreme cases. Results derived in these two cases therefore provide a qualitative insight into the extent to which anisotropy affects the contrast.

2.4. Transformation to physical coordinates

Since dimensionless integer coordinates are used in the forthcoming analysis they must be transformed to physical coordinates having dimensions. If $\mathbf{r}_{\text{phys}}$ is the vector representation of the physical coordinate our assumption that the distribution of distances between scatterers is a negative exponential implies the relation (Gandjbakhche *et al* 1992, 1993)

$$\mathbf{r}_{\text{phys}} = \frac{\mathbf{r}\sqrt{2}}{\mu_s'}. \tag{2.1}$$

To be consistent in framing the theory in terms of dimensionless units, we can also define a dimensionless time, τ, in terms of the (assumed constant) speed of light in the tissue, c, the relation being $\tau = \mu_s' ct$.

3. Definition and formalism for evaluating time-of-flight contrast

Most discussions of the idea of contrast are based on calculating the changes induced by perturbations of either the absorption or the transport-corrected scattering coefficients, μ_a and μ_s' respectively. We follow an approach to the definition of contrast first suggested in Gandjbakhche *et al* (1998), to estimate the difference in the average times to reach a given target point on the detecting surface, $\mathbf{R} = (X, Y, L)$, with and without the inclusion. Higher moments, which can, if desired (Arridge 2000), be used to improve the discrimination between the two cases, can also be evaluated by extending the formalism described in the present paper since the moments are derived in terms of derivatives of a Laplace transform whose form will be derived. These, however, require a more detailed knowledge of the pausing-time densities than assumed in the present analysis.

We first consider the case in which the times between successive steps are all equal. We ultimately want to calculate the propagator describing the trajectory of a photon initially injected at a point $\mathbf{r}_0 = (0, 0, 1)$ and detected at a point $\mathbf{R} = (X, Y, L)$ on the surface of the slab, at time τ. Denote the point adjacent to $\mathbf{R}$, but one step into the bulk of the tissue, by $\mathbf{R}_- = (X, Y, L - 1)$. This is required since, by our assumption of a simple cubic lattice structure, a photon arriving at $\mathbf{R}$ in a single step can only have come from $\mathbf{R}_-$.

The propagator in discrete time will be denoted by $p_n(\mathbf{r}|\mathbf{r}_0)$. This is the probability that the random walker, initially at $\mathbf{r}_0$, is at $\mathbf{r}$ at step n. Two further probabilities will be required in the analysis: $q_n^{(\mathbf{s})}(\mathbf{r}|\mathbf{r}')$, which is the probability that a random walker moves from $\mathbf{r}'$ to $\mathbf{r}$ in n steps, without visiting the anomalous point at $\mathbf{s}$, and $f_l^{(k)}(\mathbf{s}|\mathbf{r}_0)$, which is the probability that the random walk arrives at $\mathbf{s}$ for the kth time at step l, having started from $\mathbf{r}_0$. The two dimensionless pausing-time densities, as mentioned earlier, are $\psi_{\text{b}}(t)$ for motion on a bulk point and $\varphi_{\text{i}}(t)$ for a sojourn on an inclusion site. Later we specialize these to negative exponentials as discussed in Weiss *et al* (1998) which will serve to simplify at least some of the mathematical analyses without compromising the physical content of the theory. The physical justification for using exponential pausing time densities is based on an assumption often made in statistical physics that the distribution of scatterers in a turbid medium is negative exponential with a mean free path equal to the reciprocal of the transport-corrected scattering coefficient (Gandjbakhche and Weiss 1995).

It is worth noting that potential applications of the suggested approach are not necessarily limited to scattering perturbations. The exponential pausing time densities are also useful

in analysing fluorescence lifetime distributions generated by small fluorophores in a turbid medium (Kumar *et al* 2005). In this promising application, the rate is often all that is needed to describe a conventional lifetime distribution, i.e., one without photon migration effects because such distributions are generally described by exponentials, see, e.g., Lakowicz (1999). The theoretical approach described in this paper can help to analyse the effects of photon migration on observed lifetime intensity distributions for several different geometries, thus enabling one to estimate fluorescence lifetimes from experimental estimates of the rate as suggested below. Accurate estimates of intrinsic fluorescence fluorophores to report possible changes in such parameters as pH or temperature can therefore potentially provide valuable diagnostic information (Gannot *et al* 2004).

3.1. Enumeration of numbers of steps before reaching the target site

The definitions in the last two paragraphs enable one to derive an expression for the probability, $U^{(\mathbf{s})}_{n,k}(\mathbf{R}|\mathbf{r}_0)$, that the random walk reaches $\mathbf{R}$ at step n, having visited the inclusion at $\mathbf{s}$ exactly k times. The variable k can be any integer from 0 to n so that $U^{(\mathbf{s})}_{n,k}(\mathbf{R}|\mathbf{r}_0)$ can be represented as

$$U^{(\mathbf{s})}_{n,k}(\mathbf{R}|\mathbf{r}_0) = \gamma q^{(\mathbf{s})}_{n-1}(\mathbf{R}_-|\mathbf{r}_0)\delta_{k,0} + \gamma \sum_{l=0}^{n-1} f^{(k)}_l(\mathbf{s}|\mathbf{r}_0) q^{(\mathbf{s})}_{n-1-l}(\mathbf{R}_-|\mathbf{s}). \tag{3.1}$$

The first term on the right-hand side of this equation, $\delta_{k,0}$ being the Kronecker delta, accounts for random walks that reach $\mathbf{R}_-$ at step $n-1$, having been initially at $\mathbf{r}_0$, and not having stopped at the inclusion site at $\mathbf{s}$ during the course of the random walk. From site $\mathbf{R}_-$ it then reaches the target point $\mathbf{R}$ on the following step with probability γ. The lth term in the sum accounts for random walks that reach $\mathbf{s}$ for the kth time at step l, thereafter moving from $\mathbf{s}$ to $\mathbf{R}_-$ at step $n-1$ without returning to $\mathbf{s}$ and then moves to $\mathbf{R}$ at step n. Our ultimate goal is to find an expression for the contrast induced by the presence of the inclusion in the remaining time, and, in particular, to find a simple measure of contrast. While the n-dependent functions appearing in equation (3.1) are not easily found in a closed form, it is possible to derive expressions for their generating functions. While we have not explicitly shown the directional dependence in equation (3.1) α, β, γ probabilities appear in the q functions on the right-hand side of that equation.

The key to the calculation is that the sum over l on the right-hand side of equation (3.1) is a discrete convolution which suggests introducing a generating function with respect to n to transform the summation into a product of two generating functions. A second step in this process is to convert the discrete-time relation in equation (3.1) into a relation in continuous time. We first note that our object is to find the joint probability for the occurrence of exactly k visits to $\mathbf{s}$ with a subsequent arrival at $\mathbf{R}$ at some time during the time interval $(\tau, \tau + \mathrm{d}\tau)$ at step n. Since all n and $k \leqslant n$ can occur, we finally sum over all possible values of these variables.

We introduce notation for the pausing time density for the sum of times spent in taking l steps on all sites other than at the inclusion at $\mathbf{s}$. This will be denoted by $\psi_{\mathrm{b},l}(\tau)$ which is the probability density for the sum of l times spent on sites in the bulk. If $\hat{\psi}_{\mathrm{b}}(\xi)$ denotes the Laplace transform of the probability density for a single sojourn time on any point in the bulk, i.e., $\hat{\psi}_{\mathrm{b}}(\xi) = \int_0^\infty \psi_{\mathrm{b}}(t)\,\mathrm{e}^{-\xi t}\,\mathrm{d}t$, then a standard result in probability theory is that the Laplace transform for the probability density for the sum of l sojourns is $\hat{\psi}_{\mathrm{b},l}(\xi) = [\hat{\psi}_{\mathrm{b}}(\xi)]^l$. Similarly, the density for the sum of times spent in making l visits to the site $\mathbf{s}$ will be denoted by $\varphi_{\mathrm{i},l}(\tau)$ whose transform is $[\hat{\varphi}_{\mathrm{i}}(\xi)]^l$.

We will want to convert the relation in equation (3.1), which describes the evolution of the system in discrete time, to one which evolves in continuous time. Let the required function

be denoted by $U^{(\mathbf{s})}_{n,k}(\mathbf{R};\tau|\mathbf{r}_0)$ so that $U^{(\mathbf{s})}_{n,k}(\mathbf{R};\tau|\mathbf{r}_0)\,\mathrm{d}\tau$ is the probability that the random walk reaches $\mathbf{R}$ at a time between τ and $\tau+\mathrm{d}\tau$, having visited the inclusion at $\mathbf{s}$ exactly k times. When $k=0$

$$U^{(\mathbf{s})}_{n,0}(\mathbf{R};\tau|\mathbf{r}_0)=\gamma q^{(\mathbf{s})}_{n-1}(\mathbf{R}_-|\mathbf{r}_0)\psi_{\mathrm{b},n}(\tau) \tag{3.2}$$

which is the probability that the random walker is absorbed at $\mathbf{R}$ at time τ, never having visited the anomalous point. To generalize this to $k\geqslant 1$ we enumerate all possible trajectories, finding

$$U^{(\mathbf{s})}_{n,k}(\mathbf{R};\tau|\mathbf{r}_0)=\gamma\sum_{l=0}^{n-1}f^{(k)}_l(\mathbf{s}|\mathbf{r}_0)q^{(\mathbf{s})}_{n-1-l}(\mathbf{R}_-|\mathbf{s})\int_0^\tau\varphi_{\mathrm{i},k}(\tau')\psi_{\mathrm{b},n-k}(\tau-\tau')\,\mathrm{d}\tau',\quad k\geqslant 1. \tag{3.3}$$

As a next step in dealing with the sum in this equation we take the Laplace transform of the $U^{(\mathbf{s})}_{n,k}(\mathbf{R};\tau|\mathbf{r}_0)$. These yield the results

$$\begin{aligned}\hat{U}^{(\mathbf{s})}_{n,0}(\mathbf{R};\xi|\mathbf{r}_0)&=\gamma q^{(\mathbf{s})}_{n-1}(\mathbf{R}_-|\mathbf{r}_0)[\hat{\psi}_\mathrm{b}(\xi)]^n\\ \hat{U}^{(\mathbf{s})}_{n,k}(\mathbf{R};\xi|\mathbf{r}_0)&=\gamma\sum_{l=0}^{n-1}f^{(k)}_l(\mathbf{s}|\mathbf{r}_0)q^{(\mathbf{s})}_{n-1-l}(\mathbf{R}_-|\mathbf{s})[\hat{\varphi}_\mathrm{i}(\xi)]^k[\hat{\psi}_\mathrm{b}(\xi)]^{n-k},\quad k\geqslant 1.\end{aligned} \tag{3.4}$$

The sum with respect to n of equation (3.4) is readily found by observing that

$$S_k=\gamma\sum_{n=0}^{\infty}[\hat{\psi}_\mathrm{b}(\xi)]^n\left\{q^{(\mathbf{s})}_{n-1}(\mathbf{R}_-|\mathbf{r}_0)\delta_{n,0}+\sum_{l=0,k\geqslant 1}^{n}f^{(k)}_l(\mathbf{s}|\mathbf{r}_0)q^{(\mathbf{s})}_{n-l-1}(\mathbf{R}_-|\mathbf{s})\left(\frac{\varphi_\mathrm{i}(\xi)}{\hat{\psi}_\mathrm{b}(\xi)}\right)^k\right\} \tag{3.5}$$

is a generating function with respect to n, the transform parameter being equal to $\hat{\psi}_\mathrm{b}(\xi)$. If we denote a generating function formed from the set of constants $\{h_n\}$ by

$$\bar{h}(\alpha)=\sum_{n=0}^{\infty}h_n\alpha^n \tag{3.6}$$

then equation (3.5) can be rewritten as

$$S_k=\gamma\hat{\psi}_\mathrm{b}\left[\delta_{k,0}\bar{q}^{(\mathbf{s})}(\mathbf{R}_-;\hat{\psi}_\mathrm{b}|\mathbf{r}_0)+\bar{f}^{(k)}(\mathbf{s};\hat{\psi}_\mathrm{b}|\mathbf{r}_0)\bar{q}^{(\mathbf{s})}(\mathbf{R}_-;\hat{\psi}_\mathrm{b}|\mathbf{s})\left(\frac{\hat{\varphi}_\mathrm{i}}{\hat{\psi}_\mathrm{b}}\right)^k\right]. \tag{3.7}$$

As a final step in the calculation we need to sum over k. To this end we invoke the identity (Weiss 1994):

$$\bar{f}^{(k)}(\mathbf{s};\hat{\psi}_\mathrm{b}|\mathbf{r}_0)=\left(1-\frac{1}{\bar{p}(\mathbf{s};\hat{\psi}_\mathrm{b}|\mathbf{s})}\right)^{k-1}\frac{\bar{p}(\mathbf{s};\hat{\psi}_\mathrm{b}|\mathbf{r}_0)}{\bar{p}(\mathbf{s};\hat{\psi}_\mathrm{b}|\mathbf{s})} \tag{3.8}$$

which, together with equation (3.5), requires only the summation of a geometric series.

In our development we will use two generating functions to distinguish random walks which do or do not reach $\mathbf{s}$ at least once. The Laplace transform corresponding to those trajectories that reach the anomalous site at least once will be denoted by $\hat{U}^{(\mathbf{s})}_{\mathrm{anom}}(\mathbf{R};\xi|\mathbf{r}_0)$. The equivalent function when there is no inclusion will be denoted by $\hat{U}^{(\mathbf{s})}_{\mathrm{norm}}(\mathbf{R};\xi|\mathbf{r}_0)$. The first of these can be found by performing the sum over k in equation (3.7) using the representation for $\bar{f}^{(k)}(\mathbf{s};\hat{\psi}_\mathrm{b}|\mathbf{r}_0)$ given in equation (3.8). The sum is a geometric one and leads to the expression

$$\hat{U}^{(\mathbf{s})}_{\mathrm{anom}}(\mathbf{R};\xi|\mathbf{r}_0)=\gamma\hat{\psi}_\mathrm{b}\left[\bar{q}^{(\mathbf{s})}(\mathbf{R}_-;\hat{\psi}_\mathrm{b}|\mathbf{r}_0)+\frac{\hat{\varphi}_\mathrm{i}\bar{q}(\mathbf{R}_-;\hat{\psi}_\mathrm{b}|\mathbf{s})\bar{p}(\mathbf{s};\hat{\psi}_\mathrm{b}|\mathbf{r}_0)}{\bar{p}(\mathbf{s};\hat{\psi}_\mathrm{b}|\mathbf{s})(\hat{\psi}_\mathrm{b}-\hat{\varphi}_\mathrm{i})+\hat{\varphi}_\mathrm{i}}\right]. \tag{3.9}$$

When $\hat{\psi}_\mathrm{b} = \hat{\varphi}_\mathrm{i}$, this formula reduces to

$$\hat{U}^{(\mathbf{s})}_{\mathrm{norm}}(\mathbf{R};\xi|\mathbf{r}_0) = \gamma\hat{\psi}_\mathrm{b}[\bar{q}^{(\mathbf{s})}(\mathbf{R}_-;\hat{\psi}_\mathrm{b}|\mathbf{r}_0) + \bar{q}(\mathbf{R}_-;\hat{\psi}_\mathrm{b}|\mathbf{s})\bar{p}(\mathbf{s};\hat{\psi}_\mathrm{b}|\mathbf{r}_0)]. \tag{3.10}$$

The expressions in square brackets on the right-hand sides of equations (3.9) and (3.10) consist of two terms. The first of these, $\gamma\hat{\psi}_\mathrm{b}\bar{q}^{(\mathbf{s})}(\mathbf{R}_-;\hat{\psi}_\mathrm{b}|\mathbf{r}_0)$, is identical in both, and corresponds to trajectories that reach $\mathbf{R}$ without stopping at $\mathbf{s}$. The remaining term corresponds to trajectories that pass through $\mathbf{s}$ at least once before reaching $\mathbf{R}_-$. We will define the Laplace transform function of the contrast function, $\hat{C}(\mathbf{R};\xi|\mathbf{r}_0)$, to be the difference

$$\hat{C}(\mathbf{R};\xi|\mathbf{r}_0) = \hat{U}^{(\mathbf{s})}_{\mathrm{anom}}(\mathbf{R};\xi|\mathbf{r}_0) - \hat{U}^{(\mathbf{s})}_{\mathrm{norm}}(\mathbf{R};\xi|\mathbf{r}_0) \tag{3.11}$$

whose properties are considered below.

3.2. Laplace transform of the contrast function

The explicit representation of the Laplace transform of the contrast function is found from equation (3.11) to be

$$\hat{C}(\mathbf{R};\xi|\mathbf{r}_0) = \frac{\gamma\hat{\psi}_\mathrm{b}\bar{q}(\mathbf{R}_-;\hat{\psi}_\mathrm{b}|\mathbf{s})\bar{p}(\mathbf{s};\hat{\psi}_\mathrm{b}|\mathbf{r}_0)\bar{p}(\mathbf{s};\hat{\psi}_\mathrm{b}|\mathbf{s})(\hat{\psi}_\mathrm{b}-\hat{\varphi}_\mathrm{i})}{(\hat{\psi}_\mathrm{b}-\hat{\varphi}_\mathrm{i})\bar{p}(\mathbf{s};\hat{\psi}_\mathrm{b}|\mathbf{s})+\hat{\varphi}_\mathrm{i}} \tag{3.12}$$

which obviously vanishes when $\varphi_\mathrm{i}(\tau) = \psi_\mathrm{b}(\tau)$, i.e., when the lattice is uniform in terms of our definition framed as a difference in the two pausing time densities. The factors $\bar{p}(\mathbf{s};\hat{\psi}_\mathrm{b}|\mathbf{r}_0)$ and $\bar{p}(\mathbf{s};\hat{\psi}_\mathrm{b}|\mathbf{s})$ appear directly in terms of the propagator of the random walk on a homogeneous lattice. It is therefore convenient to express the conditional propagator $\bar{q}^{(\mathbf{s})}(\mathbf{R}_-;\hat{\psi}_\mathrm{b}|\mathbf{s})$ also in terms of the same propagator for the homogeneous lattice.

To do so, let $\hat{f}^{(1)}(\mathbf{s};\hat{\psi}_\mathrm{b}|\mathbf{r}')$ be the Laplace transform of the time for a photon to reach $\mathbf{s}$ for the first time, starting from $\mathbf{r}'$ and moving only on points other than the inclusion. To find the expression for $\bar{q}^{(\mathbf{s})}(\mathbf{R}_-;\hat{\psi}_\mathrm{b}|\mathbf{s})$ we return to the discrete-time domain which allows us to write the relation

$$q^{(\mathbf{s})}_n(\mathbf{R}_-|\mathbf{s}) = p_n(\mathbf{R}_-|\mathbf{s}) - \sum_{j=1}^{n} f^{(1)}_j(\mathbf{s}|\mathbf{s})\,p_{n-j}(\mathbf{R}_-|\mathbf{s}). \tag{3.13}$$

The first term on the right-hand side of this equation is the unrestricted propagator which takes the photon from $\mathbf{s}$ to $\mathbf{R}_-$ in n steps. One subtracts from this all trajectories that pass through $\mathbf{s}$ at least once before the nth step. When a trajectory passes through the site $\mathbf{s}$ on step j it automatically reverts to being described by an ordinary propagator which accounts for the term $p_{n-j}(\mathbf{R}_-|\mathbf{s})$ in the sum. The result is then to be converted into a generating function in terms of powers of $\hat{\psi}_\mathrm{b}$. This transforms equation (3.13) into

$$\bar{q}^{(\mathbf{s})}(\mathbf{R}_-;\hat{\psi}_\mathrm{b}|\mathbf{s}) = \bar{p}(\mathbf{R}_-;\hat{\psi}_\mathrm{b}|\mathbf{s})[1-\hat{f}^{(1)}(\mathbf{s};\hat{\psi}_\mathrm{b}|\mathbf{s})] = \frac{\bar{p}(\mathbf{R}_-;\hat{\psi}_\mathrm{b}|\mathbf{s})}{\bar{p}(\mathbf{s};\hat{\psi}_\mathrm{b}|\mathbf{s})} \tag{3.14}$$

where the last term on the right-hand side is a consequence of equation (A.2) in appendix A. We see, finally, that $\hat{C}(\mathbf{R};\xi|\mathbf{r}_0)$ can be expressed entirely in terms of the generating function of the propagator, $\bar{p}$, where the variable defining the generating function is taken to be $\hat{\psi}_\mathrm{b}$. The combination of equations (3.12) and (3.14) can be rearranged and expressed entirely in terms of the generating functions of the single photon propagators and the Laplace transforms of the pausing-time densities as

$$\hat{C}(\mathbf{R};\xi|\mathbf{r}_0) = \gamma\frac{\bar{p}(\mathbf{s};\hat{\psi}_\mathrm{b}|\mathbf{r}_0)\bar{p}(\mathbf{R}_-;\hat{\psi}_\mathrm{b}|\mathbf{s})(\hat{\psi}_\mathrm{b}-\hat{\varphi}_\mathrm{i})}{\hat{\varphi}_\mathrm{i}+(\hat{\psi}_\mathrm{b}-\hat{\varphi}_\mathrm{i})\bar{p}(\mathbf{s};\hat{\psi}_\mathrm{b}|\mathbf{s})}. \tag{3.15}$$

It is worth noting that the contrast function used for analysing experimental data in diffuse optical imaging is generally determined as a change in light intensity due to the presence of

an inclusion. Relative intensity distributions are more robust as input data because they are less sensitive to boundary effects as compared to absolute intensity values. Here, however, we use the theoretical formula which corresponds to absolute variations in intensity only as an intermediate equation to derive the expression for the MTOF variations resulting from the presence of an inclusion. It can be done using the absolute difference in the corresponding probabilities in the Laplace domain given in equations (3.12) or (3.15).

Although the equation for the transform of the contrast contains a considerable amount of information, it is nevertheless useful to have just a single parameter to measure the difference in the mean time-of-flight of a photon to arrive at site **R** attributable to the inclusion at **s**. This can be done using the absolute difference as found from the Laplace domain given later in equation (3.18). This will have the dimensions of time and will be denoted by $\Delta T(\mathbf{R})$. We define it in terms of the Laplace transform of the contrast function, $\hat{C}(\mathbf{R};\xi)$, by

$$\Delta T(\mathbf{R}) = -\frac{\mathrm{d}}{\mathrm{d}\xi}\hat{C}(\mathbf{R};\xi)\bigg|_{\xi=0}. \tag{3.16}$$

To calculate this quantity we invoke the rather obvious assumption that both $\psi_{\mathrm{b}}(t)$ and $\varphi_{\mathrm{i}}(t)$ have finite first moments. These parameters are easily found from time-resolved experimental data. A simple expression, given below, relates them to characteristics of the inclusion, either the scattering perturbation or fluorescence lifetime for a fluorophore.

By way of notation the average time spent in a single sojourn on a bulk site will be denoted by τ_{b} and the average sojourn time on the site of the inclusion by τ_{i}. This allows us to expand $\hat{\psi}_{\mathrm{b}}$ and $\hat{\varphi}_{\mathrm{i}}$ in the neighbourhood of $\xi = 0$ as

$$\hat{\psi}_{\mathrm{b}}(\xi) \approx 1 - \tau_{\mathrm{b}}\xi, \qquad \hat{\varphi}_{\mathrm{i}}(\xi) \approx 1 - \tau_{\mathrm{i}}\xi. \tag{3.17}$$

Hence, to lowest order in ξ we have

$$\frac{\Delta T(\mathbf{R})}{(\tau_{\mathrm{i}} - \tau_{\mathrm{b}})} = \gamma\,\bar{p}(\mathbf{s};1|\mathbf{r}_0)\,\bar{p}(\mathbf{R}_-;1|\mathbf{s}). \tag{3.18}$$

The right-hand side of this equation is dimensionless and contains quantities that refer only to the geometry that describes the system. While we have phrased the present problem in terms of the transillumination geometry, this is no real restriction, and it may be applied to reflectance measurements as well. Exact, but rather tedious to evaluate series for the generating functions that appear in equation (3.18) are given in appendix B. Extremely accurate integral approximations for these functions, requiring only the physically realistic condition $L \gg z_0$ are given as equations (B.10) and (B.11) of that appendix.

The dependence of the result in equation (3.18) on the two mean residence times, τ_{i} and τ_{b}, is intuitively reasonable. When these times are equal the contrast vanishes, and when a photon tends to remain at a bulk point for a time longer than at the inclusion the contrast is negative as is obvious from the physics. In the case of a scattering perturbation $\Delta\tau = \tau_{\mathrm{i}} - \tau_{\mathrm{b}}$ is proportional to the difference in scattering lengths

$$\Delta\tau \propto (\mu_s')_{\mathrm{i}}^{-1} - (\mu_s')_{\mathrm{b}}^{-1} \tag{3.19}$$

while in the case of an embedded small fluorophore it is simply the fluorescence lifetime.

The result of the present analysis is expected to be valid when the scattering coefficient is much greater than the absorption coefficient, which is very often the case with normal biological tissues in red and near-infrared light (the so-called therapeutic window, $\lambda = 650$–1100 nm, cf recent reviews, Taroni *et al* (2002), Gibson *et al* (2005)). When this condition does not hold the use of a diffusion or a random walk model may itself be called into question.

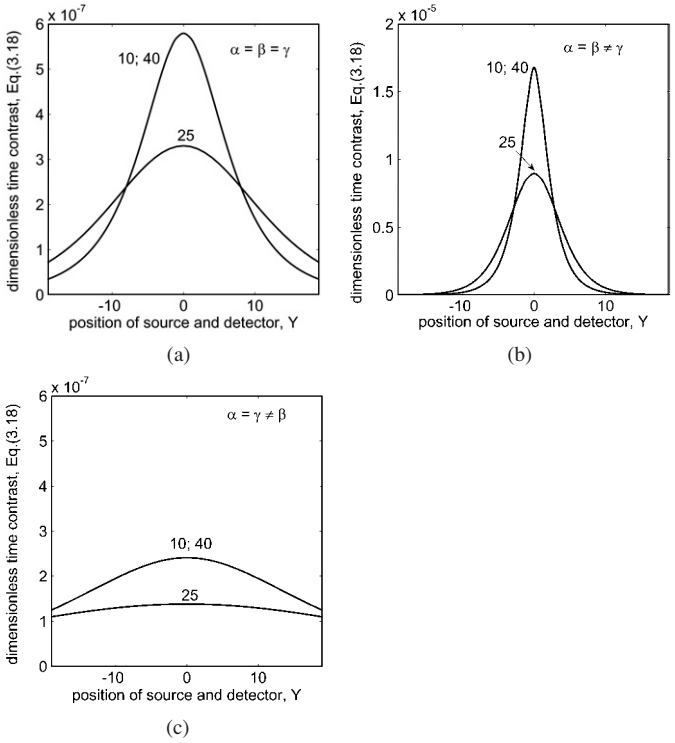

Figure 2. The contrast as defined by equation (3.18) for three values of the depth, s_z (indicated near the curves) for the configuration in which the source and detector are moved simultaneously. In the source trajectory X and Z are held fixed and motion is along Y indicated by the line $\{X = 0, Y, Z = 0\}$. Similarly, the detector trajectory is $\{X = 0, Y, Z = L\}$. In this configuration the two depths, $s_z = (L/5)$ and $s_z = (4L/5)$ of the inclusion relative to the centre of the slab have indistinguishable effects. The parameter values used to generate the curves were $L = 50$, $z_0 = 1$ and (a) $\alpha = \beta = \gamma = 1/6$; (b) case 1: $\alpha = \beta = 0.05$, $\gamma = 0.4$; (c) case 2: $\alpha = \gamma = 0.05$, $\beta = 0.4$.

To this point our analysis has been approximate, depending only on the first moments as indicated by the expansion in equation (3.17). To develop more exact expressions for the functions appearing in equation (3.18) we propose the specific *ansatz*

$$\psi_{\mathrm{b}}(t) = \frac{1}{\tau_{\mathrm{b}}} \exp\left(-\frac{t}{\tau_{\mathrm{b}}}\right), \qquad \varphi_{\mathrm{i}}(t) = \frac{1}{\tau_{\mathrm{i}}} \exp\left(-\frac{t}{\tau_{\mathrm{i}}}\right) \tag{3.20}$$

whose transforms have properties that agree with those of equation (3.17). The use of these densities enables us to calculate the functions that appear in equation (3.18). Details of the derivation are given in appendix B.

3.3. Dependence of time contrast on location of the inclusion and type of optical anisotropy

In a typical transillumination experiment the source and detector are simultaneously moved along the two surfaces so that the line connecting them is perpendicular to the two surfaces. Figure 2 shows the contrast, $\Delta T(\mathbf{R})/(\tau_i - \tau_b)$, as found from equation (3.18), as a function of the source and detector position (in the present case, X) for three different values of the inclusion depth and for two cases of optical anisotropy. In this collinear configuration it is impossible to distinguish between the cases in which the inclusion is nearer to the source or

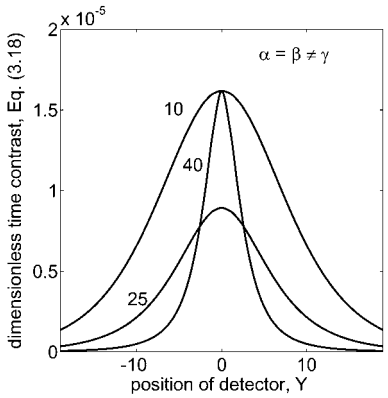

Figure 3. The contrast as defined by the MTOF in equation (3.18) for three values of the depth, s_z (indicated near the curves) for the configuration in which the source and inclusion are collinear and stationary, while the detector alone scans along the line defined by $\{X = 0, Y, Z = L\}$. This configuration, in contrast to the one defined in figure 2, allows a distinction to be made between the two depths, $s_z = (L/5)$ and $s_z = (4L/5)$ of the inclusion symmetric relative to the centre of the slab. The parameter values used to generate the curves were $L = 50$, $z_0 = 1$, $\alpha = \beta = 0.05$, $\gamma = 0.4$.

to the detecting surface as can be seen by comparing figures 2(b) and (c). Another striking difference in the generated curves is in the order of magnitudes of the contrasts in figures 2(a) and (c) as compared with 2(b). The contrast is 30 times greater in figure 2(b) than in figures 2(a) and (c) for the chosen bias and fibre orientation, because the largest transition probability moves the photon perpendicular to the surface of the slab, which maximizes the chance of the photon leaving the slab in a fixed amount of time.

A second possible configuration, leading to a qualitatively richer picture, consists of the detector being moved along the slab surface, while the source is held fixed. It is evident from figure 3 that in this configuration the depth of the inclusion can be determined unambiguously from the contrast distributions. This case can be realized, for example, when area detection, based on a CCD camera, is used. As is intuitively obvious the contrast reaches a maximum when the source, detector and inclusion lie along the same line perpendicular to the surfaces.

It is intuitively obvious that the anisotropy also must have an effect on the contrast. A comparison of the solid and dashed curves in figures 2 and 3 indicates that $\Delta T(\mathbf{R})/(\tau_i - \tau_b)$ is more localized in space when the anomalous direction is perpendicular to the slab surface ($\alpha = \beta \neq \gamma$) than when it is parallel to the slab surface.

3.4. The distributed detector measurement

So far we have assumed that the detector consists of a single point. The distributed detector measurement provides a single MTOF change integrated over the exit plane. This is not, strictly speaking, a contrast. It can nevertheless be used to verify the consistency of the model. The formalism can be generalized to deal with the case in which the detector consists of an arbitrary set of points. An example of such a generalization is the one when the detected intensity consists of photons that reach every point on the surface $z = L$. An analysis of this case requires that the coefficient in equation (3.18) be summed over all values of X and Y. This step of the analysis requires the sum (Abramowitz and Stegun 1971) $\sum_{X=-\infty}^{\infty} I_X(2\alpha\theta) = \exp(2\alpha\theta)$. Therefore, in case 1 when $\alpha = \beta \neq \gamma$ the functions $\Gamma_l(x - x', y - y')$ given in appendix B

are to be replaced by

$$\sum_{X=-\infty}^{\infty}\sum_{Y=-\infty}^{\infty}\Gamma_l(X,Y) = 4\pi^2\int_0^{\infty}\exp\left[\left(4\alpha - 1 + 2\gamma\cos\left(\frac{\pi l}{L}\right)\right)\theta\right]\mathrm{d}\theta$$

$$= \frac{\pi^2}{\gamma}\csc^2\left(\frac{\pi l}{2L}\right) \tag{3.21}$$

which is to be used in finding the generating functions of the Laplace transforms as is done earlier in this section in the context of single points.

It is clearly possible to extend this technique to deal with detectors at finite sets of points which do correspond to implementable experiments, but the resulting output might not be in as neat a mathematical form as the two examples considered so far. A further extension of the present theory replaces the single inclusion site at **s** by a set of inclusion sites. Investigations along these lines were outlined in Rubin and Weiss (1982), Weiss and Gandjbakhche (1997), but a much more elaborate analysis is required to derive useful results from the general formalism.

4. Conclusions

The principal results of our paper are the time contrast, $\Delta T(\mathbf{R})$, whose expression is given in equation (3.18), and the auxiliary functions $\Gamma_l(x - x', y - y')$ required to calculate $\bar{p}(\mathbf{r}; 1|\mathbf{r}')$ for the two orientations of the fibre structure responsible for anisotropy considered in the present paper ($\alpha = \beta \neq \gamma$ and $\alpha = \gamma \neq \beta$). Details of these functions are given in appendix B. An analysis that allows for a continuum of configurations can be developed by basing the theory on a diffusion model as in Dudko and Weiss (2005).

We have presented a tentative approach to the analysis of time-resolved data from transillumination measurements to estimate optical parameters (scattering perturbations or fluorescence lifetimes) of small inclusions or fluorophores inside turbid tissue samples. It partially accounts for anisotropic effects by allowing for fibrous structure either parallel to, or perpendicular to, the sample surface. A suggested procedure for estimating the fluorescence lifetime or the scattering perturbation consists of several steps.

(a) The inclusion is localized by analysing the time-resolved intensity distributions found by scanning the surfaces of the sample by a source–detector tandem. In the case of an increased scattering perturbation or lifetime of the fluorophore, lateral coordinates of the inclusion are determined from the position of the maximum of the MTOF of the photons, while in the case of an inclusion that induces decreased scattering these would correspond to the minimum of the MTOF of the photons. Estimation of the depth of the inclusion requires independent scans with different relative source–detector positions involving oblique angle source–detector geometry (Gandjbakhche *et al* 2003). All of the data collection can be carried out using area detection by a streak camera in combination with scanning by the source fibre over the entry plane of the sample.

(b) Optical characteristics of the background can be estimated from the intensity distributions of the time-of-flight at locations far from the inclusion fitted to either a diffusion or a random walk model (Gandjbakhche *et al* 2003).

(c) When optical properties of the background and positions of the source, detector and inclusion are known, equation (3.18) can be calculated from equations (B.10) and (B.11), allowing one to estimate the change in the MTOF of a photon due to the inclusion. This can, for example, be used to estimate the fluorescence lifetime. The latter parameter

can, under certain conditions, be used to characterize certain physical conditions (pH, temperature, etc) in the vicinity of deeply embedded inclusions and thus can provide useful diagnostic information.

It is worth noting that our suggested quantification procedure is based on a relatively robust parameter, the MTOF, and can easily be modified to deal with other configurations, e.g., reflection, by choosing in equation (3.18) the appropriate propagator describing photon migration.

Although we have dealt with only a simple model for the inclusion consisting of a single site, more complicated configurations can be dealt with using the formalism developed in Rubin and Weiss (1982) and applied in the optical context in Weiss and Gandjbakhche (1997).

Acknowledgments

This research was supported in part by the Intramural Research Programs of the National Institute of Child Health and Development and the Center for Information Technology, NIH.

Appendix A. Derivation of the generating function $\bar{p}(\mathbf{R}_-; \hat{\psi}_b|\mathbf{s})$

The function under consideration, defined essentially in equation (3.7) is

$$\bar{p}(\mathbf{R}_-; \hat{\psi}_b|\mathbf{s}) = \sum_{n=0}^{\infty}\sum_{k=0}^{n} U_{n,k}^{(\mathbf{s})}(\mathbf{R}; \xi|\mathbf{s})$$

$$= \gamma \sum_{n=0}^{\infty} \hat{\psi}_b^n(\xi) \sum_{k=0}^{n}\sum_{l=0}^{n-1} f_l^{(k)}(\mathbf{s}|\mathbf{s}) q_{n-1-l}^{(\mathbf{s})}(\mathbf{R}_-|\mathbf{s}) \left(\frac{\hat{\varphi}_i(\xi)}{\hat{\psi}_b(\xi)}\right)^k. \tag{A.1}$$

The only difference between this and the result of summing equation (3.4) is the replacement of $f_l^{(k)}(\mathbf{s}|\mathbf{r}_0)$ in that equation by $f_l^{(k)}(\mathbf{s}|\mathbf{s})$ in the present one. We therefore consider the structure of the latter function. When $l = 0$ we have $f_0^{(k)}(\mathbf{s}|\mathbf{s}) = \delta_{k,0}$.

The structure of equation (A.1) indicates that we are interested in calculating a generating function with respect to n. To evaluate this function we begin by setting $k = 1$. A well-known result in the random walk theory is (Weiss 1994)

$$\bar{f}^{(1)}(\mathbf{s}; \hat{\psi}_b|\mathbf{s}) = 1 - \frac{1}{\bar{p}(\mathbf{s}; \hat{\psi}_b|\mathbf{s})}. \tag{A.2}$$

Having this result in hand we can evaluate the remaining functions $\bar{f}^{(k)}(\mathbf{s}; \hat{\psi}_b|\mathbf{s})$ for $k \geqslant 1$ by iteration since

$$f_n^{(k+1)}(\mathbf{s}; \hat{\psi}_b|\mathbf{s}) = \sum_{l=0}^{n} f_l^{(k)}(\mathbf{s}; \hat{\psi}_b|\mathbf{s}) f_{n-l}^{(1)}(\mathbf{s}; \hat{\psi}_b|\mathbf{s}). \tag{A.3}$$

In the generating function domain this translates into $\bar{f}^{(k+1)} = \bar{f}^{(k)}\bar{f}^{(1)}$, omitting the arguments, so that

$$\bar{f}_{n,k}(\mathbf{s}; \hat{\psi}_b|\mathbf{s}) = \left[1 - \frac{1}{\bar{p}(\mathbf{s}; \hat{\psi}_b|\mathbf{s})}\right]^k \tag{A.4}$$

which is the analogue of equation (3.8) provided that the initial point is $\mathbf{s}$ rather than $\mathbf{r}_0$.

Appendix B. Generating functions for the propagators

Case 1. Anomalous direction perpendicular to the slab surface ($\alpha = \beta \neq \gamma$)

A significant feature of the results derived in the last subsection is that they can all be expressed in terms of the generating function of the discrete-time propagator as well as Laplace transforms of the pausing-time densities that define the CTRW. We provide an expression for the desired generating function by recalling that in discrete time the propagator for a nearest-neighbour random walk in a slab with absorbing boundaries at $z = 0$ and $z = L$, takes the form: (Weiss 1994)

$$p_n(\mathbf{r}|\mathbf{r}') = \frac{1}{2\pi^2 L}\sum_{l=1}^{L-1}\sin\left(\frac{\pi l z}{L}\right)\sin\left(\frac{\pi l z'}{L}\right)\int_{-\pi}^{\pi}\int \lambda_l^n(\omega_1,\omega_2) \times \cos[\omega_1(x-x')]\cos[\omega_2(y-y')]\,\mathrm{d}\omega_1\,\mathrm{d}\omega_2 \tag{B.1}$$

in which

$$\lambda_l(\omega_1,\omega_2) = 2\alpha(\cos\omega_1 + \cos\omega_2) + 2\gamma\cos\left(\frac{\pi l}{L}\right) \tag{B.2}$$

which is just a characteristic function associated with the random walk in discrete time. Since, in finding $\bar{p}(\mathbf{r}|\mathbf{r}')$ the bracketed term must be raised to the nth power, we need only to sum a geometric series to find that the required characteristic function has the form

$$\bar{p}(\mathbf{r};1|\mathbf{r}') = \frac{1}{2\pi^2 L}\sum_{l=1}^{L-1}\sin\left(\frac{\pi l z}{L}\right)\sin\left(\frac{\pi l z'}{L}\right)\Gamma_l(x-x',y-y') \tag{B.3}$$

where

$$\Gamma_l(x-x',y-y') = \int_{-\pi}^{\pi}\int \frac{\cos[\omega_1(x-x')]+\cos[\omega_2(y-y')]}{1-\lambda_l(\omega_1,\omega_2)}\,\mathrm{d}\omega_1\,\mathrm{d}\omega_2. \tag{B.4}$$

To simplify the double integral we invoke the identity $u^{-1} = \int_0^\infty \exp(-u\theta)\,\mathrm{d}\theta$ which transforms the expression for $\Gamma_l(x-x',y-y')$ to

$$\Gamma_l(x-x',y-y') = \int_0^\infty \mathrm{e}^{-u}\,\mathrm{d}u\int_0^\infty \{\cos[\omega_1(x-x')]+\cos[\omega_2(y-y')]\} \times \exp u\left[2\alpha(\cos\omega_1+\cos\omega_2)+2\gamma\cos\left(\frac{\pi l}{L}\right)\right]\mathrm{d}\omega_1\,\mathrm{d}\omega_2. \tag{B.5}$$

The integrals with respect to the ω's are proportional to modified Bessel functions of the first kind (Abramowitz and Stegun 1971), since, for example,

$$\int_{-\pi}^{\pi}\cos[\omega(x-x')]\exp(-2\alpha\xi\cos\omega)\,\mathrm{d}\omega = 2\pi I_{x-x'}(2\alpha\xi) \tag{B.6}$$

so that $\Gamma_l(x-x',y-y')$ can be expressed in the form of a Laplace transform:

$$\Gamma_l(x-x',y-y') = 4\pi^2\int_0^\infty I_{x-x'}(2\alpha\xi)I_{y-y'}(2\alpha\xi)\exp\left(-\left\{1-2\gamma\cos\left[\frac{\pi l}{L}\right]\right\}\xi\right)\mathrm{d}\xi \tag{B.7}$$

which is easily evaluated numerically or else can be written in terms of a hypergeometric function whose exact form is somewhat complicated (Roberts and Kaufman 1966).

Case 2. Anomalous direction parallel to the slab surface ($\alpha = \gamma \neq \beta$)

An important distinction to be made between the present and the earlier configuration is that contours of equal intensity on the detecting surface are elliptical, as opposed to being circular

(Dagdug *et al* 2003). The mathematical formalism for case 2 differs only slightly from that used in dealing with the case 1. The major difference is that $\lambda_l(\omega_1, \omega_2)$ in equation (B.2) is now to be replaced by

$$\lambda_l(\omega_1, \omega_2) = 2\alpha\left[\cos\omega_1 + \cos\left(\frac{\pi l}{L}\right)\right] + 2\beta\cos\omega_2. \tag{B.8}$$

The further analysis proceeds exactly as in case 1 except for the slight modification required in the calculation of $\Gamma_l(x - x', y - y')$ required by the last equation. A similar analysis leads to

$$\Gamma_l(x - x', y - y') = 4\pi^2\int_0^\infty I_{x-x'}(2\alpha\xi)I_{y-y'}(2\beta\xi)\exp\left[-\left\{1 - 2\alpha\cos\left(\frac{\pi l}{L}\right)\right\}\xi\right]\mathrm{d}\xi. \tag{B.9}$$

As is true for the function Γ_l given in equation (B.2) an exact expression for the resulting integral in terms of a hypergeometric function can be found but is not useful for generating numerical results.

While equation (B.3) is exact, it requires rather extensive numerical calculations which can be avoided by noting that it will quite generally be true that $L \gg 1$ allowing us to derive an accurate approximation in this limiting case. Consider case 1 as defined above. We pass to the limit of an integral by defining the variable $\eta = \pi l/L$, in which case we can write

$$\begin{aligned}\bar{p}(\mathbf{r}; 1|\mathbf{r}') &\approx \frac{2}{\pi}\int_0^\pi \sin(\eta z)\sin(\eta z')\,\mathrm{d}\eta \\ &\quad\times\int_0^\infty I_{x-x'}(2\alpha\xi)I_{y-y'}(2\alpha\xi)\exp(-\{1 - 2\gamma\cos\eta\}\xi)\,\mathrm{d}\xi \\ &= \int_0^\infty \mathrm{e}^{-\xi}I_{x-x'}(2\alpha\xi)I_{y-y'}(2\alpha\xi)[I_{z-z'}(2\gamma\xi) - I_{z+z'}(2\gamma\xi)]\,\mathrm{d}\xi.\end{aligned} \tag{B.10}$$

In a similar fashion in case 2, $\alpha = \gamma \neq \beta$, equation (B.9) can be used to approximate to the sum for $\bar{p}(\mathbf{r}; 1|\mathbf{r}')$ by

$$\begin{aligned}\bar{p}(\mathbf{r}; 1|\mathbf{r}') &\approx \frac{2}{\pi}\int_0^\pi \sin(\eta z)\sin(\eta z')\,\mathrm{d}\eta \\ &\quad\times\int_0^\infty I_{x-x'}(2\alpha\xi)I_{y-y'}(2\beta\xi)\exp(-\{1 - 2\alpha\cos\eta\}\xi)\,\mathrm{d}\xi \\ &= \int_0^\infty \mathrm{e}^{-\xi}I_{x-x'}(2\alpha\xi)I_{y-y'}(2\beta\xi)[I_{z-z'}(2\alpha\xi) - I_{z+z'}(2\alpha\xi)]\,\mathrm{d}\xi.\end{aligned} \tag{B.11}$$

References

Abramowitz M and Stegun I A 1971 *Handbook of Mathematical Functions* (New York: Dover)

Arridge S R 1995 Photon-measurement density functions: I. Analytical forms *Appl. Opt.* **34** 7395–409

Arridge S R, Hebden J C, Schwinger M, Schmidt F E W, Fry M E, Hillman E M C, Dehghani H and Delpy D T 2000 A method for three-dimensional time-resolved optical tomography *Int. J. Imaging Syst. Technol.* **11** 2–11

Binzoni T, Courvoisier C, Giust R, Tribillon G, Gharbi T, Hebden J C, Leung T S, Roux J and Delpy D T 2006 Anisotropic photon migration in human skeletal muscle *Phys. Med. Biol.* **51** N79–90

Chernomordik V, Hattery D W, Gannot I, Zaccanti G and Gandjbakhche A H 2002 Analytical calculation of the mean time spent by photons inside an absorption inclusion embedded in a highly scattering medium *J. Biomed. Opt.* **7** 486–92

Dagdug L, Weiss G H and Gandjbakhche A H 2003 Effects of anisotropic optical properties on photon migration in structured tissues *Phys. Med. Biol.* **48** 1361–70

Dudko O K and Weiss G H 2005 Estimation of anisotropic optical parameters in a slab geometry *Biophys. J.* **88** 3205–11

Gandjbakhche A H, Bonner R F, Chernomordik V, Hebden J C and Nossal R 1998 Time-dependent contrast functions for quantitative imaging in time-resolved transillumination experiments *Appl. Opt.* **37** 1973–81

Gandjbakhche A H, Bonner R F and Nossal R 1992 Scaling relations for anisotropic random walks *J. Stat. Phys.* **69** 35–53

Gandjbakhche A H, Bonner R F and Nossal R 1993 Scaling relations for theories of anisotropic random walks applied to tissue optics *Appl. Opt.* **32** 504–16

Gandjbakhche A H, Bonner R F, Nossal R and Weiss G H 1996 Absorptivity contrast in transillumination imaging of tissue abnormalities *Appl. Opt.* **35** 1767–74

Gandjbakhche A H, Chernomordik V, Hattery D, Hassan M and Gannot I 2003 Tissue characterization by quantitative optical imaging methods *Techn. Canc. Res. Treat.* **2** 537–51

Gandjbakhche A H, Nossal R and Bonner R F 1994 Resolution limits for optical parameters for optical transillumination of abnormalities embedded in tissues *Med. Phys.* **22** 185–91

Gandjbakhche A H and Weiss G H 1995 Random walk and diffusion-like models of photon migration in turbid media *Prog. Opt.* **34** 335–402

Gannot I, Ron I, Hekmat F, Chernormordik V and Gandjbakhche A H 2004 Functional optical detection based on pH dependent fluorescence lifetimes *Lasers Surg. Med.* **35** 342–8

Gibson A P, Hebden J C and Arridge S R 2005 Recent advances in diffuse optical imaging *Phys. Med. Biol.* **50** R1–43

Hebden J C 1999 Simultaneous reconstruction of absorption of absorption and scattering images by multichannel images by multichannel measurement of purely temporal data *Opt. Lett.* **24** 534–6

Hebden J C and Arridge S R 1996 Imaging through scattering media by the use of an analytical model of perturbation amplitudes in the time domain *Appl. Opt.* **35** 6788–96

Hebden J C, Guerrero J J G, Chernomordik V and Gandjbakhche A H 2004 Experimental evaluation of an anisotropic scattering model of a slab geometry *Opt. Lett.* **29** 2518–20

Heino J, Arridge S and Sommersalo E 2002 Anisotropic effect in light scattering and some implications in optical tomography *Tech. Dig. OSA Biomed. Topical Meetings* pp 18–20

Hughes B D 1995 *Random Walks and Random Environments,* vol 1: *Random Walks* (Oxford: Clarendon)

Kaltenbach J M and Kaschke M 1993 Frequency- and time-domain modelling of light transport in random media *Medical Optical Tomography: Functional Imaging and Monitoring* ed G Muller vol IS11 p 65

Kienle A, Forster F K, Diebolder R and Hibst R 2003 Light propagation in dentin: influence of microstructure on anisotropy *Phys. Med. Biol.* **48** N7–14

Kumar A T N, Skoch J, Bacskai B J, Boas D A and Dunn A K 2005 Fluorescence-lifetime-based tomography for turbid media *Opt. Lett.* **30** 3347–9

Lakowicz J R 1999 *Principles of Fluorescence Spectroscopy* 2nd edn (New York: Kluwer/Plenum)

Michielsen K, De Raedt H, Przeslawski J and Garcia N 1998 Computer simulation of time-resolved optical imaging of objects hidden in turbid media *Phys. Rep.* **304** 89–144

Morin M, Verreault S, Mailloux A, Fréchette J, Chatigny S, Painchaud Y and Beaudry P 2000 Inclusion characterization in a scattering slab with time-resolved transmittance measurements *Appl. Opt.* **39** 2840–52

Nickell S, Herman M, Ehrenpreis M, Farrell T J, Krämer U and Patterson M S 2000 Anisotropy of light propagation in human skin *Phys. Med. Biol.* **45** 2873–6

Painchaud Y, Mailloux A, Morin M, Verrault S and Beaudry P 1999 Time-domain optical imaging: distinction between scattering and absorption *Appl. Opt.* **38** 3686–93

Roberts G E and Kaufman H 1966 *Table of Laplace Transforms* (Philadelphia, PA: Saunders)

Rubin R J and Weiss G H 1982 Random walks on lattices. The problem of visits to a set of points revisited *J. Math. Phys.* **23** 250–3

Sviridov A, Chernomordik V, Eidsath A, Hassan A G and Gandjbakhche A H 2005 Intensity profiles of linearly polarized light backscattered from skin and tissue-like phantoms *J. Biomed. Opt.* **10** C1D04012

Taroni P 2002 Time-resolved spectroscopy and imaging in diffusive media applied to medical diagnostics *Riv. Nuovo Cimento* **25** 1–19

Weiss G H 1994 *Aspects and Applications of the Random Walk* (Amsterdam: North-Holland)

Weiss G H and Calabrese P P 1996 Occupation times of a CTRW on a lattice *Physica* A **234** 443–54

Weiss G H and Gandjbakhche A H 1997 Effects of nonlocalized target shape in the random walk description of transillumination experiments *Phys. Rev.* E **56** 3451–9

Weiss G H, Porrà J M and Masoliver J 1998 The continuous-time random walk description of photon motion in an isotropic medium *Opt. Commun.* **146** 268–76